Repositorio Institucional de la Universidad Autónoma de Madrid

https://repositorio.uam.es

Esta es la **versión de autor** del artículo publicado en:
This is an **author produced version** of a paper published in:

Sensors and Actuators, B: Chemical 222 (2016): 331-338

DOI: https://doi.org/10.1016/j.snb.2015.08.033

Copyright: © 2015 Elsevier B.V. All rights reserved.

El acceso a la versión del editor puede requerir la suscripción del recurso

Access to the published version may require subscription

Insulin Sensor Based on Nanoparticle-Decorated Multiwalled Carbon Nanotubes Modified Electrodes

Emiliano Martínez-Periñán[a], Mónica Revenga-Parra[a], Marcelo Gennari[b], Félix Pariente[a], Rubén Mas-Ballesté[b], Félix Zamora[b,c], Encarnación Lorenzo[a,c,*]

[a]Departamento de Química Analítica, Universidad Autónoma de Madrid, 28049 Madrid, Spain

[b]Departamento de Química Inorgánica, Universidad Autónoma de Madrid, 28049 Madrid, Spain

[c]IMDEA-Nanoscience. Faraday 9, Campus Cantoblanco-UAM, 28049 Madrid, Spain

*Corresponding author. Tel.: +34 91 497 4488; fax: +34 91 497 4931.

E-mail address: encarnacion.lorenzo@uam.es (E. Lorenzo)

Postal address: Facultad de Ciencias. c/ Francisco Tomás y Valiente, 7. Departamento de Química Analítica y Análisis Instrumental. Universidad Autónoma de Madrid, 28049, Madrid, Spain.

Abstract

Insulin sensors based on glassy carbon electrodes, modified with nafion-multiwalled carbon nanotubes decorated with nickel hydroxide nanoparticles (Ni(OH)$_2$NPs/Nafion-MWCNTs/GC), were prepared by electrochemical deposition of Ni(OH)$_2$NPs from a dinuclear paddle-wheel Ni monothiocarboxylate complex on the MWCNTs/GC surface. The size and distribution of the

Ni(OH)$_2$NPs/Nafion-MWCNTs were characterized by transmission electron microscopy (TEM). The results show that Ni(OH)$_2$ nanoparticles were electrodeposited on the surface of carbon nanotubes. Moreover, the electrochemical behavior of the modified electrodes in aqueous alkaline solutions of insulin was studied by cyclic voltammetry and chronoamperometry. It was found that the as prepared nanoparticles have excellent electrocatalytic activity towards insulin oxidation due to their special properties, reducing the overpotential and improving the electrochemical behavior, compared to the bare GC electrode. Amperometry was used to evaluate the analytical performance of modified electrode in the determination of insulin. Excellent analytical features, including high sensitivity (5.0 A mol cm^{-2} µM^{-1}), low detection limit (85 nM) and wide dynamic range (up to 10.00 µM), were achieved under optimum conditions. Moreover, these insulin sensors show good repeatability and a high stability after successive potential cycling. Common substances such as ascorbic acid, uric acid and acetaminophen do not interfere. Finally, they have been applied to the determination of insulin in pharmaceuticals and in human plasma. Efficient recoveries for pharmaceuticals and human plasma demonstrate that the proposed methodology can be satisfactorily applied to these types of samples.

Keywords

Dinickel complexes, paddle-wheel complexes, nickel hydroxide nanoparticles, insulin electrocatalysis.

1. Introduction

Diabetes is caused by the insufficient release of insulin or loss of insulin action at target tissues, which results in aberrant glucose and lipid metabolism. Insulin is an important polypeptide hormone produced in the pancreas that is used to control the glucose levels in blood within a narrow concentration range [1,2]. The administration of insulin constitutes the fundamental treatment of the diabetes mellitus type 1. Although we have insulin for more than 75 years, in the last two decades important changes have been realized due to the use of biosynthetic human insulins, which are obtained by means of technologies of genetic recombination from cultures of bacteria (*Escherichia coli*) or yeasts. Recently, it has also started using insulin analogous either of much rapid (Aspart) or slow action (Glargine). The detection of insulin is of great importance not only for clinical diagnostics, because it serves as a predictor of diabetes of insulinoma and trauma [3,4] but also for drug quality and prescription.

Many different analytical methods have been described for the quantitative analysis of insulin, among them radioimmunoassay [5,6], fluorescence resonance energy transfer (FRET) [7], MALDI-TOF mass spectrometry [8], capillary electrophoresis [9], HPLC [10], etc. However, most of these methods are time-consuming, cumbersome, and expensive. As resulting, although detection of this analyte possesses many challenges, as far as we know, no commonly accepted reference method for insulin determination has been yet established and the scientist community is making an effort in order to establish one.

The use of electrochemical methods, in particular electrochemical sensor, offers some advantages compared to other methodologies, such as high sensitivity, rapid response, low cost, miniaturization and more important the possibility to construct portable devices easy to use for point of care. It enables real time monitoring, which could be a real improved in prediabetes individuals diagnosis. However, electrochemical sensors as an analytical tool for insulin determination require the use of modified electrodes because the direct oxidation of insulin at conventional electrodes is limited by a low sensitivity, reproducibility, selectivity and signal stability. This is largely due to the high

overpotential at which the insulin oxidation process takes place, slow kinetics and surface electrode fouling [11]. Modified electrodes have been successfully used for insulin determination. Among different modifying agents used to avoid the mentioned problems, it can be mentioned: ruthenium oxide film [12], cobalt oxide nanoparticles [13], silica nanoparticles [14], iridium oxide [15], nickel oxide nanoparticles [16].

The new trends in insulin electrochemical sensors development combine organic or inorganic redox mediators with nanostructures, in particular different carbon nanomaterials such as graphene nanosheets and mostly carbon nanotubes have been employed [16-18]. The great advantage of use carbon nanotubes is they enable negligible surface fouling [19], which is one of the principal problems that affects electrochemical sensors based on sulfur groups oxidation [20].

During the last decades there has been an increase interest in the development of new non-noble metal base catalyst and electrocatalyst, which has led the use of nickel and cobalt compounds. Both, nickel and cobalt metal centers are of particular interest as redox mediators in basic media showing high catalytic activity towards the electroxidation of organic compounds containing hydroxyl groups and sulfur derivatives. In the case of nickel, the electrocatalytic effect is considered to arise from unpaired d electrons or empty d orbitals associated with the oxidized form of Ni, which are available for bond formation with adsorbed species or redox intermediates [21-23]. On the other hand, for electrocatalytic applications, catalytic activity increases significantly moving from bulk materials to nanosized structures. Thus, the use of supporting substrates decorated with nanoparticles or nanostructures can be a good strategy to create highly efficient electrocatalyst [14,16,24,25]. In this sense, it is well known that high-surface-area CNT combined with metal nanoparticles or metal oxides can improve the performance of the final material [26]. Indeed, modified electrodes with a suitable electrocatalyst (Ni^{2+}/Ni^{3+} redox couple), combined with carbon nanomaterials, in order to avoid fouling effects, has been successfully employed to electrocatalyze insulin oxidation [11,16-18].

Different chemical routes, such as sonochemistry, sol gel, and solvothermal methods, among others, [27-34] have been described for the formation of nickel hydroxide on surfaces. However, these methods typically result in thin film structures [35-38]. The direct formation of particles in situ on the electrode of interest represents a simpler alternative. Furthermore, as amply demonstrated for the formation of immobilized metal nanostructures, the size and coverage of electrodeposited nanostructures can be modulated controlling the electrode potential [39].

Previous reported studies of nickel hydroxide electrodeposition have in general focused on either the electrochemical generation of OH^- in the presence of Ni^{2+} to form directly nickel hydroxide [40-42] or an indirect approach in which nickel is first electrodeposited from Ni^{2+} in solution or a nickel metal electrode is employed and the nickel is fully oxidized by potential cycling in strong alkaline solution [43-46]. There are no reports in the literature concerning the production of isolated nickel hydroxide nanoparticles on whatever electrode surface by the direct approach; rather, thin film structures tend to be produced. Only randomly isolated nickel hydroxide nanoparticles have been formed on boron-doped diamond electrodes [47]. The indirect approach generally results in the formation of predominantly micrometer-sized nickel hydroxide particles [48,49] and a heterogeneous surface distribution.

We have recently described a novel method for the production of highly-dense and uniform surface coverages of isolated $Ni(OH)_2$ nanoparticles of small size (≈ 10 nm) on different electrode surfaces [50]. In this work, since the method developed is an interesting route for the production of high coverages of $Ni(OH)_2$ as isolated NPs on different electrode surfaces, we have gone a step further and we have employed them to decorate CNTs, due to large specific surface area and high electrical conductivity of this nanomaterial. Moreover, combining the above mentioned excellent properties of CNTs, as well as antifouling material, with the high electrocatalytic activity and special properties of the $Ni(OH)_2$

nanoparticles generated, we have used the resulting hybrid nanomaterial for the development of an insulin electrochemical sensor.

2. Experimental

2.1. Reagents and apparatus

Dinuclear Ni monothioacetate paddle-wheel complex, $[Ni_2(CH_3COS)_4 \cdot EtOH]$, was prepared according to a slight literature modification [51]. A warm ethanolic solution of thioacetic acid (0,037 mol) was treated with $[NiCO_3 \cdot 2Ni(OH)_2 \cdot 4H_2O]$ (0,018 mol) in a portion-wise fashion. Color changed from light orange to deep red in about 30 min and the mixture was stirred further for 4h. The suspension formed was filtered and the precipitated discarded, filtrate was allowed to stand overnight at -10 ºC to yield deep red plate-like crystals, 1.854 g (43 %). ^{1}H NMR spectra were recorded on a Bruker AMX-300 spectrometer. C, H, S elemental analyses were performed on a Perkin-Elmer 240-B microanalyser.

Carboxylated Multiwall carbon nanotubes (>95% carbon purity) (MWCNT-COOH) were obtained from Nanocyl S.A. Their average diameter is 9.5 nm and their average length is about 1.5 μm. Stock dispersions containing 1.0 mg mL^{-1} of MWCNTs-COOH were prepared in a 0.005% Nafion Milli-Q water solution by sonication during 1h in an ultrasonic bath.

5% Nafion solution, bovine pancreas insulin (27 units/mg), tetrabutyl ammonium perchlorate (TBAP) electrochemical grade, dry chloroform ($CHCl_3$) and sodium hydroxide were purchased from Sigma Aldrich. Stock solutions containing 0.5 mM of insulin were freshly prepared daily in 0.1 M NaOH aqueous solution. Some insulin formulations obtained as pharmaceutical preparations, Insulin Glargine (Lantus® SoloStar®, 100 U/mL, Sanofi-Aventis) and Insulin Aspart (NovoRapid® FlexPen®, 100 U/mL, NovoNordisk), and human plasma obtaining from healthy volunteers were used for the analytical application.

Cyclic voltammetry and amperometry were used to study the electrocatalytic properties and the response of the Ni(OH)$_2$NPs/Nafion-MWCNTs/GC modified electrode. All electrochemical measurements were carried out using an Autolab potentiostat/galvanostat type PGSTAT 302N (Eco

Chemie, Netherlands) using the software package GPES 4.9. A homemade three electrodes electrochemical cell was used for electrochemical experiments. Glassy Carbon (GC) disk electrode (3 mm diameter) for CH Instruments was used as working electrode and a platinum wire as counter electrode. Homemade Calomel electrode was used as reference electrode for aqueous solutions. Special Calomel electrode for organic medium from Radiometer Analytical was used for electrochemical experiments in chloroform solutions. Rotating disk electrode (RDE) measurements were carried out using a Glassy Carbon disk electrode from PINE. All experiments were made at room temperature.

For the nanoscale catalysts characterization by transmission electron microscopy (TEM), gold grids were used and images were recorded with a JEOL JEM 2100 electron microscope.

2.2. Procedures

2.2.1. Preparation of Ni(OH)$_2$NPs/Nafion-MWCNTs/GC modified electrode.

Prior to the electrode modification, the glassy carbon surface was polished to a mirror-like surface with 0.1 µm of diamond paste in a Buelher polishing cloth with ultrapure water as lubricant. After thoroughly rinsing, 5 µL of MWCNTs-COOH stock dispersion were casted onto the surface of GC electrodes and were dried at ambient conditions. Ni(OH)$_2$ nanoparticles were generated along the MWCNT modified glassy carbon electrode following the method developed by us [50]. Briefly it is based on the electrogeneration of [Ni$_2$(CH$_3$COO)$_4$] microstructures from a solution containing 0.1 mM of the dinickel paddle-wheel complex [Ni$_2$(CH$_3$COS)$_4$·EtOH] in 0.1 M TBAP/CHCl$_3$ by applying 1.15 V during 150 s. Then, the modified electrodes were rinsed with chloroform and immersed in 0.1 M NaOH solutions. Finally, 50 potential cycles between 0.0 and +0.7 V at 0.1 V s^{-1} were applied to obtain Ni(OH)$_2$NPs/Nafion-MWCNTs/GC modified electrodes.

For TEM measurements, the layer of carbon nanotubes decorated with Ni(OH)$_2$ nanoparticles was removed from the GC electrode and dispersed in 100 µL of pure acetone. 5 µL of the suspension was deposited onto the gold grid and led to dry in a desiccator.

2.2.2. Determination of insulin in pharmaceuticals and in human plasma.

Prior to use, both samples were purified using Amicon® Ultra 3K centrifugal filter (Millipore) and then diluted in 0.1 M NaOH solution. The standard addition method was used for quantitative analysis.

3. Results and discussion

3.1. Preparation of Ni(OH)₂NPs/Nafion-MWCNTs/GC modified electrode

Ni(OH)$_2$NPs have been directly electrogenerated on glassy carbon electrodes modified with MWCNTs dispersed in Nafion as is described in the experimental section. The influence of precursor concentration ([Ni$_2$(CH$_3$COS)$_4$·EtOH]), potential and time on the electrodeposition of Ni microstructures ([Ni$_2$(CH$_3$COO)$_4$]) is a crucial step on the size and surface coverage of the resulting Ni(OH)$_2$NPs. Therefore, it was evaluated. Best results were obtained when 0.1 mM of precursor was electrodeposited at 1.15 V during 150 s.

TEM has been employed for the morphological characterization of the resulting Ni(OH)$_2$NPs/Nafion-MWCNTs/GC modified electrode. As can be observed in the TEM images of the nanocrystalline Ni(OH)$_2$ decorated MWCNTs (Fig. 1), Ni(OH)$_2$NPs are distributed on the Nafion-MWCNTs surface in the form of single sticks. This confirms that Ni(OH)$_2$NPs can therefore grow by electrodeposition into the Nafion-MWCNT matrix. It can be also deduced from this image that although some aggregation of the Ni(OH)$_2$NPs occurs, nanoparticles have almost a narrow size distribution (≈10 nm) arranged in the framework of Nafion-MWCNTs.

The deposition of quite dispersed nanoparticles on Nafion-MWCNTs is believed to be as result of the uniform surface functional sites present along the nanotube, such as carboxylic acid groups. During the surface modification process, the surface oxides may act as active sites in the electrodeposition of nickel compounds. Within the period selected for the electrodeposition, the particles grow to an equivalent size, in different particle densities over the surface of MWCNTs.

Figure 1.

3.2. Electrochemical behavior of Ni(OH)₂NPs/Nafion-MWCNTs/GC electrodes

The electrochemical behavior of as prepared Ni(OH)₂NPs/Nafion-MWCNTs/GC electrode was studied in 0.1 M NaOH. Successive cyclic voltammetry scans are shown in Fig. 2. As can be observed the shape of the voltammogram changes after the first scan and then remains constant showing a well-defined redox-couple with a formal potential of +0.39 V, which correspond to the widely reported process:

Oxidation peak:

$$Ni(OH)_2 \rightarrow NiOOH + e^- + H^+$$

Reduction peak:

$$NiOOH + e^- + H^+ \rightarrow Ni(OH)_2$$
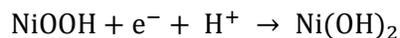
The surface coverage (Γ) can be evaluated from the cyclic voltammograms by using the equation $\Gamma = Q_{Ox} / nFA$, where Q_{Ox} is the charge obtained after integration of the oxidation peak, F is the Faraday constant (96485 C mol^{-1}), n is the number of electrons transferred in the redox process (n = 1) and A is the area of the electrode (0.07 cm^2). The Γ value was calculated to be 2.26 x 10^{-8} mol cm^{-2}. This value is about 10 times higher than that obtained when no MWCNTs were used [50]. The stability of the Ni(OH)₂NPs/Nafion-MWCNTs/GC electrode was evaluated from cyclic voltammograms obtained under continuous potential cycling from 0.0 to +0.7 V at 0.1 V s^{-1} in 0.1 M NaOH. As can be seen in Fig. 2, the very slow shift of oxidation peak potential observed during electrochemical cycling suggests a gradual conversion of Ni^{2+} to Ni^{3+}. Moreover a significant decay in the current was observed during the first scan. However after this initial loss of electroactive material, the additional loss was less than 7% for continuous cycling during 10 min. The resulting modified electrodes exhibit an excellent stability and high Ni(OH)₂NPs surface coverage.

Figure 2.

The electrogenerated $Ni(OH)_2$ exhibited the voltammetric shape typical of oxidized surfaces and the significant ΔEp is typical of such process. In fact, counterion transport can be limiting and thus the large ΔEp value [52]. The formal potential (E=+0.45 V) is practically constant at low scan rates and the anodic and cathodic peak currents show a linear dependence with the square root of the sweep rate over the range of 0.02–0.75 V s^{-1} as anticipated for a diffusion controlled process; again likely counterion transport (Fig. 3A). These results indicate that, at low scan rates the system is electrochemically quasi-reversible suggesting facile charge transfer kinetics. At high scan rates, the value of ΔEp increases. This electrochemical irreversibility is indicative of serious limitations in the kinetics of charge transfer at these conditions. Although the Laviron's formalism is generally applicable to simple redox reactions, and in this case counterion transport could be rate limiting, taking into account that the redox species are immobilized on the electrode surface, the apparent surface electron-transfer rate constant (k_s), as well as the electron-transfer coefficient (α) were determined through the Laviron's equations [53]. The anodic and cathodic peak potentials were plotted *vs* log (v) in a typical Laviron's plot (Fig. 3B). At scan rates higher than 4 V s^{-1} the peak potential depicts a linear dependence with log (v) (Fig. 3C). From the ratio of the slopes of these straight lines, the electron transfer coefficient (α) and the apparent surface electron-transfer rate constant (k_s) were found to be 0.49 and 22.9 s^{-1}, respectively.

Figure 3.

3.3. Electrocatalysis of insulin oxidation

Direct oxidation of insulin represents an interesting method for the determination of this compound in a fast and easy way. Fig. 4B shows cyclic voltammograms recorded at a $Ni(OH)_2NPs/Nafion$-MWCNTs/GC modified electrode in the absence and in the presence of 0.5 mM insulin. In the absence of insulin the redox couple ascribed to the Ni^{2+}/Ni^{3+} process is evident. Upon addition of

insulin, an increase in the anodic peak current concomitant with a decrease in the cathodic current is observed. This behavior is characteristic of an electrocatalytic effect and indicates that $Ni(OH)_2NPs$ directly participate in the oxidation of insulin, which causes a decrease in the number of Ni(III) centers and the consequently decrease in the cathodic current in the backward scan. In addition, a shift of the peak potential to more positive potentials is observed. This fact may be due to a kinetic limitation in the electroxidation process. These results were compared to those obtained in the absence of $Ni(OH)_2NPs$, at a Nafion-MWCNTs/GC modified electrode (Fig. 4A). In this case, in the presence of insulin an adsorption peak at approximately +0.24 V appears. Successive additions of insulin show that the current is not linearly related to concentration (data not shown).

An advantage of using the $Ni(OH)_2NPs$/Nafion-MWCNTs/GC electrode prepared by us, compared to other similar modified electrodes [16], is that with our Ni modified electrode the presence of insulin causes the increase of the anodic peak current of the Ni^{2+}/Ni^{3+} redox couple instead of the appearance of a new one at higher potential. This fact may be due to the better and faster electron transfer communication between our $Ni(OH)_2$ nanoparticles based redox system and the analyte (insulin).

Figure 4.

In order to obtain the better electrocatalytic efficiency towards insulin oxidation, the electrodeposition time and the concentration of the precursor $[Ni_2(CH_3COS)_4 \cdot EtOH]$ for the electrode modification were optimized. For this purpose, the concentration of the precursor in the electrodeposition step was varied from 0.05 to 0.20 mM in 0.1 M TBAP/CHCl$_3$, which was performed at a constant potential of 1.15 V during 150 s. The electrocatalytic efficiency was estimated as the ratio i_{CAT}/i_D; where i_{CAT} and i_D are the currents in the presence or in the absence of insulin. From these results it can be concluded that the better efficiency (1.15) was obtained employing 0.1 mM of precursor. Once the concentration of precursor was optimized, we optimized

the electrodeposition time applying a constant potential of 1.15 V during different times. The optimum value was found to be 150 s. From the above results we have selected the following conditions to decorated Nafion-MWCNT/ GC electrodes with Ni(OH)$_2$NPs: 0.1mM of precursor in 0.1M TBAP/CHCl$_3$ applying 1.15 V during 150 s.

3.4. Determination of the catalytic rate constant

The effect of the potential scan rate in the electrocatalytic response to 0.5 mM insulin in 0.1 M NaOH solutions was also evaluated. The catalytic current increases linearly with the square root of scan rates in the range of 0.01-0.5 V s^{-1} (inset, Fig. 5). This means that the insulin electroxidation process is diffusion controlled. However, as can be seen in Fig. 5, the anodic peak potential shifts towards positive potentials as the scan rate increases, which suggests that the process has a kinetic limitation.

Figure 5.

The catalytic rate constant has been determined by the method described by Galus [54], using cronoamperometric measurements. This method is based on the equation:

$$\frac{i_{CAT}}{i_D} = \gamma^{1/2}\left[erf(\gamma^{1/2}) + \frac{\exp(-\gamma)}{\gamma^{1/2}}\right]$$

i_{CAT} and i_D are the currents in the presence and absence of insulin respectively. γ is the argument of the error function described as $\gamma = kC^*t$, where C^* is the bulk concentration of insulin in the solution and k is the catalytic rate constant and t is the elapsed time in seconds. The catalytic rate constant as a function of insulin concentration was estimated by plotting i_{CAT}/i_D *vs* the square root of time. From the slope of a secondary plot we have determined a catalytic rate constant of $(1.12 \pm 0.01) \times 10^3$ M^{-1} s^{-1}. This quite high value confirms that the method developed gives rise nanoparticles with a very high catalytic efficiency.

3.5. Insulin sensor response

To prove the potential application of these efficient electrocatalyst as an insulin sensor, the amperometric response of electrocatalyst-modified electrodes to increasing concentrations of insulin was assayed.

Fig. 6A depicts the chronoamperograms recorded under quiescent conditions (unstirred solution) to ensure the diffusion control. The potential is pulsed from 0.00 V to +0.50 V, and the corresponding current transients are recorded in the presence of increasing concentrations of insulin. As can be seen, the steady state current (i_{ss}) stabilizes after a few seconds. A plot of i_{ss} *vs* $C_{insulin}$ is linear (inset, Fig. 6A) within the concentration range of 1.50-40.0 µM with a correlation coefficient of 0.995 and a sensitivity of 1.1 A mol cm^{-2} µM^{-1}, revealing that Ni(OH)$_2$NPs/Nafion-MWCNTs/GC modified electrodes can be used as insulin sensors. The analytical properties were obtained from the slope of the calibration curve obtained under Cottrell experimental conditions. The detection and quantification limits, calculated as the concentration of insulin that gave a signal equal to three and ten times the standard deviation of background current, were found to be 0.44 and 1.5 µM, respectively. The reproducibility was evaluated from three different sensors for 20.0 µM insulin determination. The average response was 19.2 µM with a standard deviation of 0.52 µM (R.S.D. 2.7 %). Concerning the stability, we have employed the same modified electrode during the course of a day in numerous insulin determinations such as a complete calibration (in replicate determinations). After an initial loss of activity (10 %), the modified electrode exhibited a very stable response during hours of continuous work. As an example, in replicate determinations (n = 3) of 40.0 µM insulin, we observed less than 10% of loss of activity. This behavior indicates that insulin or its oxidation products do not block the Ni(OH)$_2$NPs/Nafion-MWCNTs/GC modified electrode surface. Moreover, an electrode can be employed after dry storage condition for 60 days at room temperature in air with a loss of activity of about 9%. However, due to the ease of preparation we typically modified an electrode and employed it in all determinations in the course of a day.

Figure 6.

Considering the fact that chronoamperometric measurements carried out under stirring conditions are expected to give a better sensitivity than calibration curves obtained under quiescent solutions, a new calibration curve was carried out using a $Ni(OH)_2NPs/Nafion-MWCNTs/GC$ rotating disk electrode. Fig. 6B shows the amperometric response of a $Ni(OH)_2NPs/Nafion-MWCNTs/GCRDE$ to successive additions of insulin. A plot of i_{ss} *vs* insulin concentration is linear (inset, Fig. 6B) up to 10.0 µM with a correlation coefficient of 0.9899 and a sensitivity of 5.0 A mol cm^{-2} $µM^{-1}$. The detection and quantification limits, calculated as is described above, were found to be 85 and 490 nM, respectively. These values are comparable to those previously described for similar insulin sensor [11,17,55] and are adequate to the direct determination of insulin in different matrix such us pharmaceutical o biological fluids.

The reproducibility was evaluated from three different sensors for 1.50 µM insulin determination. The average response was 1.497 µM with a standard deviation of 0.065 µM (R.S.D. 4.3 %).

3.6. Interference study

One of the most important aspects to take into account for any analytical application of sensors is the study of the effect of interfering compounds potentially present in the real sample. In order to evaluate the possible interfering effect of few common substances, the sensor response for 5.0 µM insulin was obtained in the absence and in presence of different concentrations of ascorbic acid, uric acid, acetaminophen and glucose under the optimized experimental conditions (Table 1). The presence of the potential interfering compounds did not affect the response except in the case of glucose where an increase of about 19% of the signal was observed. However, at lower concentrations the presence of this compound did not show any effect. These results agree well with the presence of Nafion in the sensor, which avoids the interference of negative charged compounds such as ascorbate.

Table 1. Interference tests on various compounds for the assay of insulin.

Compound	Relative response* (%)	
	[insulin]:[interference]	
	1:1	1:0.1
Ascorbic acid	39	3
Uric acid	45	0.7
Acetoaminophen	50	4
Glucose	119	7

*The solution contains 5.0 µM insulin and the response compared to that of plain 5.0 µM insulin taken as 100%.

3.7. *Determination of insulin in pharmaceuticals and in human plasma*

The insulin sensor developed was applied to the determination of insulin in pharmaceuticals, in particular two commercial injections containing insulin analogous of rapid (Aspart) and slow action (Glargine), and in human plasma. For this purpose, prior the determination both samples were purified as is described in the experimental section. In the case of pharmaceuticals, amperometric data recorded during analysis of unspiked samples showed a linear increase of the current with increasing insulin concentrations. The recovery and precision of the complete method were evaluated and the results are shown in Table 2. On the other hand, when human plasma was used, a certain value of standard solution of insulin (1.8 µM) was added into the plasma for testing the recovery. As can be seen in Table 2, in this case the recovery was less efficient probably due to the complexity of the matrix.

Table 2. Determination of insulin in real samples

Sample	Spiked Value (µM)	Recovery % ± SD*
Insulin pharmaceuticals:		
NovoRapid®	0	97.2±0.6
Lantus®	0	98.4±0.3
Human plasma	1.8	80±6

*SD: Standard deviation of three determinations

4. Conclusions

Nanoestructures of Ni(OH)$_2$ with high catalytic properties toward insulin were electrodeposited on Nafion-MWCNTs/GC electrodes from a dinuclear paddle-wheel Ni monothiocarboxylate complex complex. TEM images confirm that Ni(OH)$_2$ based nanostructures were successfully electrodeposited along the surface of MWCNTs. The catalytic reaction of insulin at Ni(OH)$_2$NPs/Nafion-MWCNTs/GC modified electrodes was studied by chronoamperometry and cyclic voltammetry. From these studies the catalytic rate constant was determined to be $(1.12 \pm 0.01) \times 10^3 \ M^{-1} \ s^{-1}$. The resulting modified electrode has been shown to be effective for insulin determination with good reproducibility and long-term stability and was applied for insulin determination in human plasma and pharmaceuticals with excellent results.

Acknowledgments

References

[1]   J. Sanger, The free amino groups of insulin, Biochemical Journal. 39 (1945) 507-515.

[2]   Z. Chen, M.P. Caulfield, M.J. McPhaul, R.E. Reitz, S.W. Taylor, N.J. Clarke, Quantitative Insulin Analysis Using Liquid Chromatography–Tandem Mass Spectrometry in a High-Throughput Clinical Laboratory, Clinical Chemistry. 59 (2013) 1349-1356.

[3]   H. K. Ortmeyer, N. L. Bodkin, B. C. Hansen, Relationship of skeletal-muscle glucose-6-phosphate to glucose disposal rate and glycogen-synthase activity in insulin-resistant and non-insulin-dependent diabetic rhesus-monkeys, Diabatologia 37 (1994) 127-133.

[4]   T. G. Jenssen, I. Toft, K. H. Bonaa, Can plasma insulin/glucose ratio be used to predict insulin sensitivity, Diabatologia 38 (1995), 127A.

[5]   J.R. Lindsay, A.M. McKillop, M.H. Mooney, F.P.M. O'Harte, P.M. Bell, P.R. Flatt, Demonstration of increased concentrations of circulating glycated insulin in human Type 2 diabetes using a novel and specific radioimmunoassay, Diabetologia. 46 (2003) 475-478.

[6]   S. Moriyama, P. Swanson, M. Nishii, A. Takahashi, H. Kawauchi, W.W. Diekhoff, E.M. Plisetskaya, Development of a Homologous Radioimmunoassay for Coho Salmon Insulin-like Growth Factor-I, Gen. Comp. Endocrinol. 96 (1994) 149-161.

[7]   Y. Wang, D. Gao, P. Zhang, P. Gong, C. Chen, G. Gao, L. Cai, A near infrared fluorescence resonance energy transfer based aptamer biosensor for insulin detection in human plasma, Chem. Commun. 50 (2014) 811-813.

[8]   X. Zhang, S. Zhu, C. Deng, X. Zhang, An aptamer based on-plate microarray for high-throughput insulin detection by MALDI-TOF MS, Chem. Commun. 48 (2012) 2689-2691.

[9]   N.M. Schultz, L. Huang, R.T. Kennedy, Capillary electrophoresis-based immunoassay to determine insulin content and insulin secretion from single islets of Langerhans, Anal. Chem. 67 (1995) 924-929.

[10] M.M. Moein, M. Javanbakht, B. Akbari-adergani, Molecularly imprinted polymer cartridges coupled on-line with high performance liquid chromatography for simple and rapid analysis of human insulin in plasma and pharmaceutical formulations, Talanta. 121 (2014) 30-36.

[11] M. Zhang, C. Mullens, W. Gorski, Insulin Oxidation and Determination at Carbon Electrodes, Anal. Chem. 77 (2005) 6396-6401.

[12] W. Gorski, C.A. Aspinwall, J.R.T. Lakey, R.T. Kennedy, Ruthenium catalyst for amperometric determination of insulin at physiological pH, J. Electroanal Chem. 425 (1997) 191-199.

[13] A. Salimi, R. Hallaj, Cobalt oxide nanostructure-modified glassy carbon electrode as a highly sensitive flow injection amperometric sensor for the picomolar detection of insulin, Journal of Solid State Electrochemistry. 16 (2012) 1239-1246.

[14] N. Amini, M.B. Gholivand, M. Shamsipur, Electrocatalytic determination of traces of insulin using a novel silica nanoparticles-Nafion modified glassy carbon electrode, J Electroanal Chem. 714–715 (2014) 70-75.

[15] M. Pikulski, W. Gorski, Iridium-Based Electrocatalytic Systems for the Determination of Insulin, Anal. Chem. 72 (2000) 2696-2702.

[16] B. Rafiee, A.R. Fakhari, Electrocatalytic oxidation and determination of insulin at nickel oxide nanoparticles-multiwalled carbon nanotube modified screen printed electrode, Biosensors and Bioelectronics. 46 (2013) 130-135.

[17] A. Arvinte, A.C. Westermann, A.M. Sesay, V. Virtanen, Electrocatalytic oxidation and determination of insulin at CNT-nickel–cobalt oxide modified electrode, Sensors Actuators B: Chem. 150 (2010) 756-763.

[18] J. Wang, T. Tangkuaram, S. Loyprasert, T. Vazquez-Alvarez, W. Veerasai, P. Kanatharana, P. Thavarungkul, Electrocatalytic detection of insulin at RuOx/carbon nanotube-modified carbon electrodes, Anal. Chim. Acta. 581 (2007) 1-6.

[19] M. Pumera, The Electrochemistry of Carbon Nanotubes: Fundamentals and Applications, Chemistry, A European Journal. 15 (2009) 4970-4978.

[20] L.G. Shaidarova, A.V. Gedmina, I.A. Chelnokova, M.L. Artamonova, H.C. Budnikov, Electrocatalytic oxidation and flow-injection determination of sulfur amino acids on a glassy carbon electrode modified by a nickel(II) polytetrasulfophthalocyanine film, Journal of Analytical Chemistry. 68 (2013) 536-544.

[21] P. Cox, D. Pletcher, Electrosynthesis at oxide coated electrodes Part 1 the kinetics of ethanol oxidation at spinel electrodes in aqueous base, J. Appl. Electrochem. 20 (1990) 549-554.

[22] Y.L. Lo, B.J. Hwang, Kinetics of Ethanol Oxidation on Electroless Ni-P / SnO2 / Ti Electrodes in KOH Solutions, Journal of The Electrochemical Society. 142 (1995) 445-450.

[23] D. Pletcher, Electrocatalysis: present and future, J. Appl. Electrochem. 14 (1984) 403-415.

[24] M. Govindhan, M. Amiri, A. Chen, Au nanoparticle/graphene nanocomposite as a platform for the sensitive detection of NADH in human urine, Biosensors and Bioelectronics. 66 (2015) 474-480.

[25] S. Yang, G. Li, G. Wang, J. Zhao, M. Hu, L. Qu, A novel nonenzymatic H2O2 sensor based on cobalt hexacyanoferrate nanoparticles and graphene composite modified electrode, Sensors Actuators B: Chem. 208 (2015) 593-599.

[26] A. Arvinte, A. Sesay, V. Virtanen, Carbohydrates electrocatalytic oxidation using CNT–NiCo-oxide modified electrodes, Talanta. 84 (2011) 180-186.

[27] P. Jeevanandam, Y. Koltypin, A. Gedanken, Synthesis of nanosized alpha-nickel hydroxide by a sonochemical method, Nano Lett. 1 (2001) 263–266.

[28] B. Pejova, T. Kocareva, M. Najdoski, I. Grozdanov, A solution growth route to nanocrystalline nickel oxide thin films, Appl. Surf. Sci. 165 (2000) 271-278.

[29] M. Vidotti, R. P. Salvador, S. I. Córdoba de Torresi, Synthesis and characterization of stable Co and Cd doped nickel hydroxide nanoparticles for electrochemical applications, Ultrason. Sonochem. 16 (2009) 35-40.

[30] Y. Wang, Q. S. Zhu, H. G. Zhang, Fabrication of beta-Ni(OH)(2) and NiO hollow spheres by a facile template-free process Chem. Commun. 41 (2005) 5231-5233.

[31] L. Liu, Y. Li, S. M. Yuan, M. Ge, M.M. Ren, C. S. Sun, Z. Zhou, Nanosheet-Based NiO Microspheres: Controlled Solvothermal Synthesis and Lithium Storage Performances, J. Phys. Chem. C. 114 (2010) 251-255.

[32] S.A. Needham, G. X. Wang, H. K. Liu, Synthesis of NiO nanotubes for use as negative electrodes in lithium ion batteries, J. Power Sources 159 (2006) 254-257.

[33] G. T. Duan, W. P. Cai, Y. Y. Luo, Z. G. Li, Y. Lei, Hierarchical structured Ni nanoring and hollow sphere arrays by morphology inheritance based on ordered through-pore template and electrodeposition, J. Phys. Chem. B 110 (2006) 15729-15733.

[34] Y. L. Tai, H. S. Teng, Template synthesis and electrochemical characterization of nickel-based tubule electrode arrays, Chem. Mater. 16 (2004) 338-342.

[35] M. Vidotti, S. I. Córdoba de Torresi, Electrostatic layer-by-layer and electrophoretic depositions as methods for electrochromic nanoparticle immobilization, Electrochim. Acta 54 (2009) 2800-2804.

[36] M.S. Wu, H.H. Hsieh, Nickel oxide/hydroxide nanoplatelets synthesized by chemical precipitation for electrochemical capacitors, Electrochim. Acta 53 (2008) 3427-3435.

[37] A.A. Al-Ghamdi, W. E. Mahmoud, S.J. Yaghmour, F.M. Al-Marzouki, Structure and optical properties of nanocrystalline NiO thin film synthesized by sol–gel spin-coating method, J. Alloys Compd. 486 (2009) 9-13.

[38] A. Sawaby, M. S. Selim, S. Y. Marzouk, M. A. Mostafa, A. Hosny, Structure, optical and electrochromic properties of NiO thin films, Phys. B 405 (2010) 3412-3420.

[39] E. C. Walter, B. J. Murray, F. Favier, G. Kaltenpoth, M. Grunze, R. M. Penner, Noble and coinage metal nanowires by electrochemical step edge decoration, J. Phys. Chem. B 106 (2002) 11407-11411.

[40] G. H. A. Therese, P. V. Kamath, Electrochemical synthesis of metal oxides and hydroxides, Chem. Mater. 12 (2000) 1195-1204.

[41] Y. Tan, S. Srinivasan, K.-C. Choi, Electrochemical deposition of mesoporous nickel hydroxide films from dilute surfactant solutions, J. Am. Chem. Soc. 127 (2005) 3596-3604.

[42] C. C. Streinz, A. P. Hartman, S. Motupally, J. W. Weidner, The effect of current and nickel nitrate concentration on the deposition of nickel-hydroxide films, J. Electrochem. Soc. 142 (1995) 1084-1089.

[43] R. P. Deo, N. S. Lawrence, J. Wang, Electrochemical detection of amino acids at carbon nanotube and nickel-carbon nanotube modified electrodes, Analyst 129 (2004) 1076-1081.

[44] J. F. Huang, Facile preparation of an ultrathin nickel film coated nanoporous gold electrode with the unique catalytic activity to oxidation of glucose, Chem. Commun. 10 (2009) 1270-1272.

[45] M. Jafarian, F. Forouzandeh, I. Danaee, F. Gobal, Electrocatalytic oxidation of glucose on Ni and NiCu alloy modified glassy carbon electrode, J. Solid State Electrochem. 13 (2009) 1171–1179.

[46] M. A. Abdel Rahim, R. M. Abdel Hameed, M. W. Khalil, Nickel as a catalyst for the electro-oxidation of methanol in alkaline medium, J. Power Sources 134 (2004) 160-169.

[47] L. A. Hutton, M. Vidotti, A. N. Patel, M. E. Newton, P. R. Unwin, J. V. Macpherson, Electrodeposition of Nickel Hydroxide Nanoparticles on Boron-Doped Diamond Electrodes for Oxidative Electrocatalysis, J. Phys. Chem. C. 115 (2011) 1649-1658.

[48] N. R. Stradiotto, K. E. Toghill, L. Xiao, A. Moshar, R. G. Compton, The Fabrication and Characterization of a Nickel Nanoparticle Modified Boron Doped Diamond Electrode for Electrocatalysis of Primary Alcohol Oxidation, Electroanalysis 21 (2009) 2627-2633.

[49] Y. Chang, J. Qiao, Q. Liu, L. Shangguan, X. Ma, S. Shuang, C. Dong, Electrochemical Behavior of Hydrogen Peroxide at a Glassy Carbon Electrode Modified with Nickel Hydroxide-Decorated Multiwalled Carbon Nanotubes, Anal. Lett. 41 (2008) 3147-3160.

[50] E. Martínez-Periñán, M. Gennari, M. Revenga-Parra, J.M. Abad, E. Mateo-Martí, F. Pariente, O. Castillo, R. Mas-Ballesté, F. Zamora, E. Lorenzo, Highly-dense nickel hydroxide nanoparticles catalyst electrodeposited from a novel Ni(II) paddle-wheel complex, J. Cat (accepted).

[51] G. A. Melson, P. T. Greene, R. F. Bryan, Crystal and molecular structure of tetra-μ-thiobenzoato-dinickel(II)-ethanol, [Ni(PhCOS)$_2$]$_2$EtOH, Inorg. Chem. 9 (1970) 1116.

[52] H. B. Li, M. H. Yu, F. X. Wang, P. Liu, Y. Liang, J. Xiao, C. X. Wang, Y. X. Tong and G. W. Yang, Nat. Commun. 4 (2013) 1894.

[53] E. Laviron, General expression of the linear potential sweep voltammogram in the case of diffusionless electrochemical systems, J. Electroanal. Chem. 101 (1979) 19-28.

[54] Z. Galus, Fundamentals of Electrochemical Analysis. (1994) 520.

[55] Y. Lin, L. Hu, L. Li and K. Wang, Facile synthesis of nickel hydroxide-graphene nanocomposites for insulin detection with enhanced electro-oxidation properties, RSC Adv. 4 (2014), 46208-46213.

Figure captions

Fig. 1. TEM images of Ni(OH)$_2$NPs/Nafion-MWCNTs/GC modified electrode.

Fig. 2. Cyclic voltammograms of Ni(OH)$_2$NPs/Nafion-MWCNTs/GC modified electrode in 0.1 M NaOH at 0.1 V s^{-1}.

Fig. 3. (A) Cyclic voltammetric response of Ni(OH)$_2$NPs/Nafion-MWCNTs/GC modified electrode in 0.1 M NaOH at different scan rates. Inset B: Laviron's plot showing the dependence of the peak potential on the logarithm of scan rate. Inset C: Linear segments of the above Laviron's plot.

Fig. 4. Cyclic Voltammograms of Nafion-MWCNTs/GC (A) or Ni(OH)$_2$NPs/Nafion-MWCNTs/GC (B) electrode in 0.1 M NaOH in the absence (solid line) and in the presence of 0.5 mM of insulin (dashed line). Scan rate 0.010 V s^{-1}.

Fig. 5. Cyclic voltammograms for a Ni(OH)$_2$NPs/Nafion-MWCNTs/GC modified electrode in 0.1 M NaOH in the presence of 0.5 mM insulin, obtained at different scan rates. Inset: Linear relationship of anodic peak intensity current *vs* square root scan rate for the cyclic voltammograms depicted in the figure.

Fig. 6. Current transients (A) and current responses (B) of a Ni(OH)$_2$NPs/Nafion-MWCNTs/GC electrode (A) and a Ni(OH)$_2$NPs/Nafion-MWCNTs/GC rotating disk electrode (B) to increasing concentrations of insulin at +0.5 V in 0.1 M NaOH solution. Insets: Plots of i$_{ss}$ *vs* insulin concentrations.
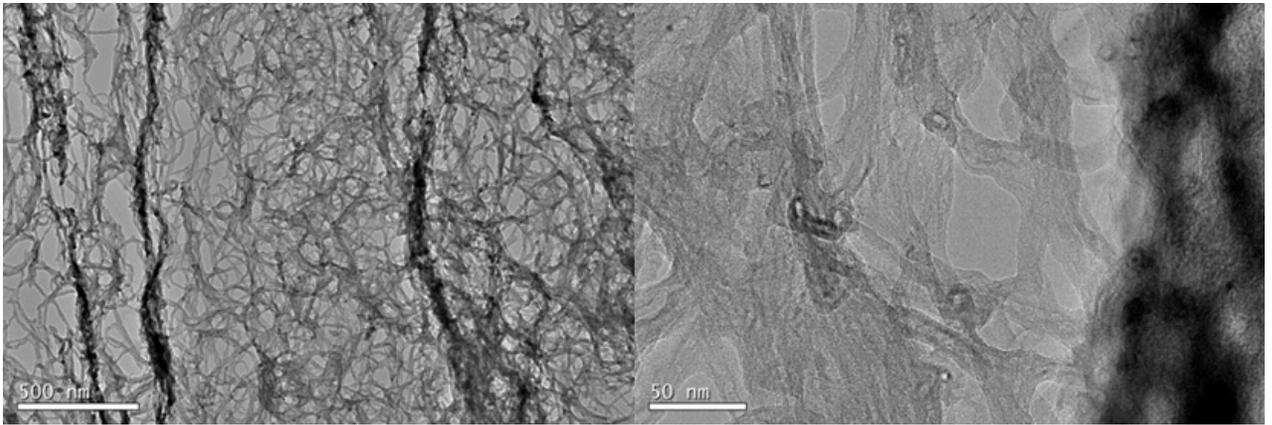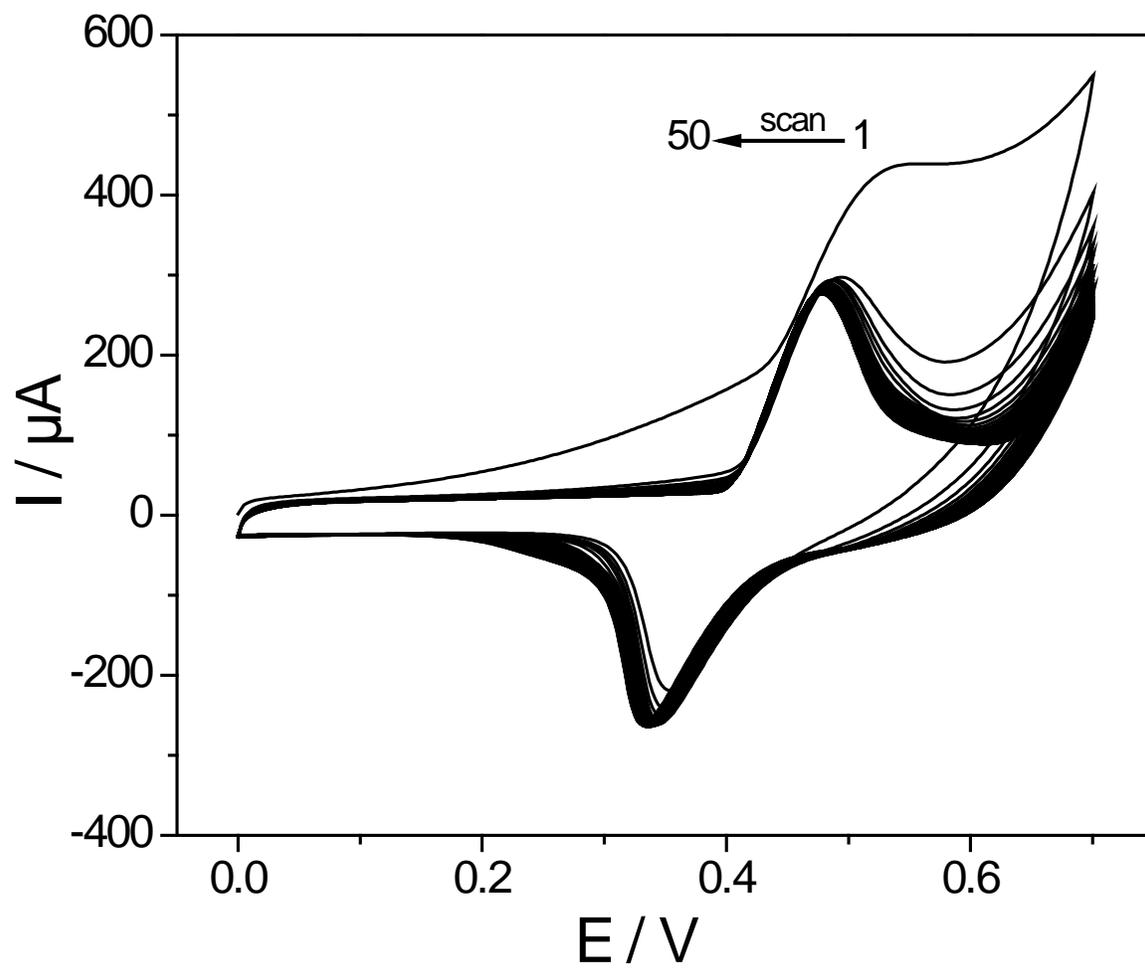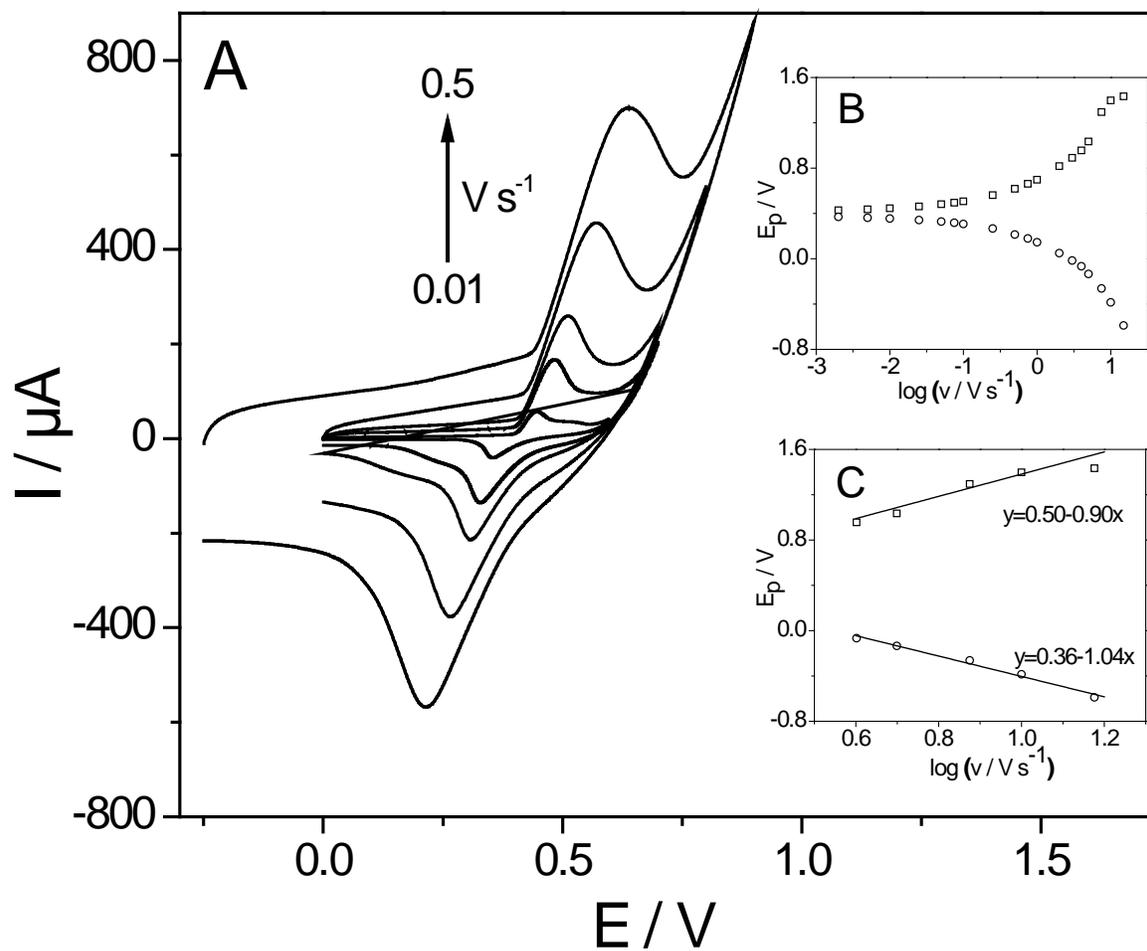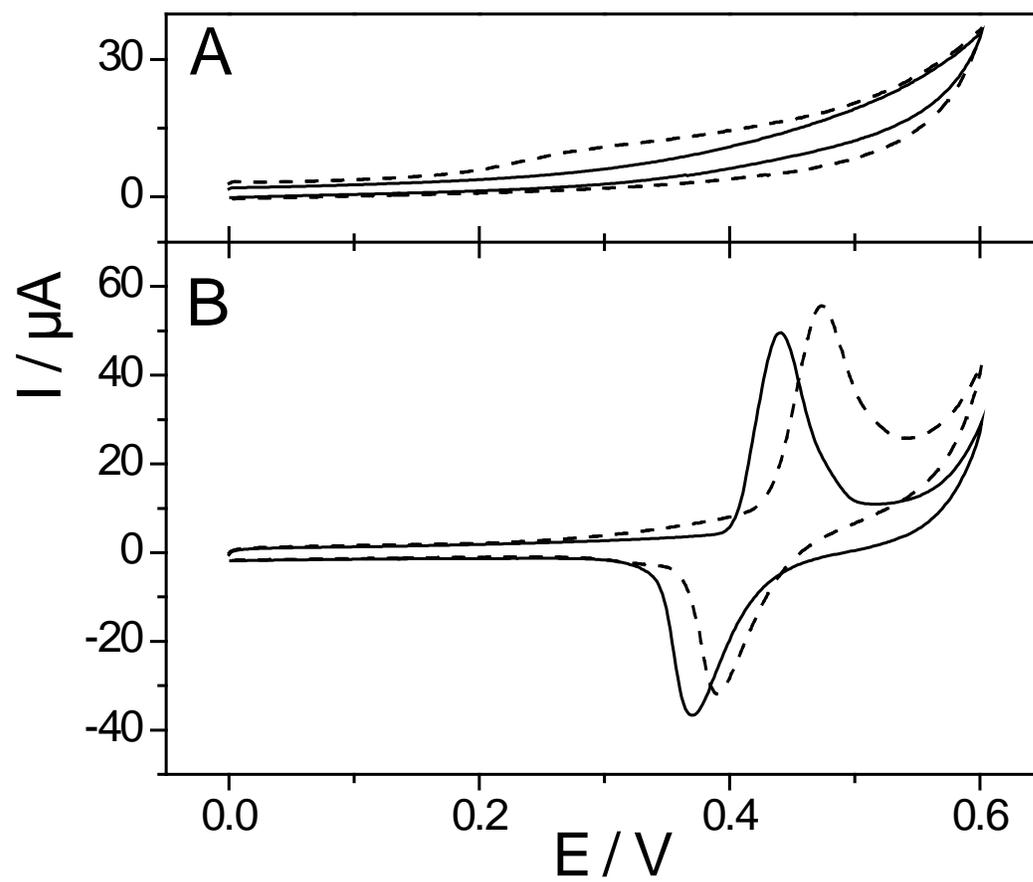
Fig. 1.

Fig. 2.

Fig. 3.

Fig. 4.

Fig. 5.

Fig. 6.